

# COMPUTER PACKAGE FOR GRAPHITE TOTAL CROSS-SECTION CALCULATIONS

**M. Adib and M. Fathalla**

*Reactor Physics Department, Nuclear Research Center ,Atomic Energy  
Authority, Cairo ,Egypt*

## Abstract

An additive formula is given which allows calculating the contribution of the total neutrons transmission through crystalline graphite. The formula takes into account the graphite form of poly or pyrolytic crystals and its parameters. Computer package GRAPHITE has been designed in order to provide the required calculations in the neutron energy range from 0.1meV to 10eV. The package includes three codes: PCG (Polycrystalline Graphite), PG (Pyrolytic Graphite) and HOPG (Highly Oriented Pyrolytic Graphite) for calculating neutron transmission through fine graphite powder (polycrystalline), neutron transmission and removal coefficient of PG crystal in terms of its mosaic spread for neutrons incident along its c-axis and the transmission of neutrons incident on HOPG crystal at different angles, respectively. For comparison of the experimental neutron transmission data with the calculated values, the program takes into consideration the effect of both wavelength and neutron beam divergence in either constant wavelength spread mode ( $\Delta\lambda=\text{constant}$ ) or constant wavelength resolution mode ( $\Delta\lambda/\lambda=\text{constant}$ ). In order to check the validity for application of computer package GRAPHITE in cross-section calculations, a comparison between calculated values with the available experimental data were carried out. An overall agreement is indicated with an accuracy sufficient for determine the neutron transmission characteristics

## INTRODUCTION

Neutron diffraction powder investigation is usually carried out with wavelengths ranging from 0.10 to 0.15 nm. Although longer wavelengths can lead to an increased resolution, their use is limited due to higher-order contamination problems. The development of the triple-axis spectrometer for inelastic neutron scattering has proved to be valuable for excitations in solids, liquids, and gases [1]. This spectrometer requires a monochromator to select single incident neutron energy and an analyzer to determine the energy of neutrons scattered from a sample. In some cases, the spectrometers are required to operate in gain energy mode [2]. Such mode simplifies the analysis of measured phonon spectrum. When using such mode the selected neutrons are of wavelengths longer than 0.4 nm (cold neutrons)[3].

It is well known that, the coherent elastic scattering by a crystalline material cannot occur for neutrons with wavelengths which exceed some maximum value of  $\lambda_{\text{max}}$ , where  $\lambda_{\text{max}}$  is given by  $\lambda_{\text{max}} = 2d_{\text{max}}$ , and  $d_{\text{max}}$  is the largest d spacing of planes in the crystal. The variation of the scattering cross-section in the vicinity of  $\lambda_{\text{max}}$  for a number of polycrystalline filters, of which Be, BeO, and graphite are perhaps the most commonly used [4]. The best filter materials will be those for which the remaining contributions to cross sections are small for  $\lambda > \lambda_{\text{max}}$ . It is known that graphite cross section beyond  $\lambda_{\text{max}}$  is the

lowest among others. Moreover, the inelastic contribution may be reduced by cooling the material to say liquid nitrogen temperature. A sufficiently thick filter will then transmit a beam of cold neutrons with little attenuation, while reducing the intensity with  $\lambda < \lambda_{\max}$  by three or four orders of magnitude.

A beam of monochromatic neutrons, selected from the spectrum of a nuclear reactor by means of diffraction by a monochromator crystal, will in general contaminate with higher-order components. When a primary wavelength larger than 0.2nm is selected, the second-order component is so important that a suitable filter becomes indispensable. When the selected neutrons is in the spectral range from 0.233 to 0.286nm (energy range between 15 and 10meV), it can lead to an increased resolution both for the study of magnetic systems and time-resolved investigation of chemical systems. In this respect, the use of PG has led to a considerable improvement in neutron diffraction techniques.

PG has been in use for about 30 years as a filter. The principle of operation is that for neutron traveling along the *c*-axis of this material, with certain neutron wavelength ( $\lambda$ ) cannot be Bragg scattered, while second-order neutrons ( $\lambda/2$ ) are strongly scattered. This differs considerably from polycrystalline graphite in which all neutron energies above the lowest Bragg cut-off at approximately 0.0018eV are strongly scattered.

Since in PG, crystallites are preferentially oriented along the hexagonal *c*-axis. The transmission of neutrons thru PG with *c*-axis parallel to the beam versus neutron wavelength, exhibits "absorption" lines due to Bragg scattering. These lines are responsible for selective removal of  $\lambda/2$ ,  $\lambda/3$ ,... neutrons from the beam. The width of the lines is restricted by angular spread of the *c*-axes. It is therefore expected that a reduction in the angular spread of *c* axes in a PG filter will lead to reduction in the transmissions of  $\lambda/2$ ,  $\lambda/3$ ,... neutrons without significantly affecting the transmission of  $\lambda$  neutrons.

Frikkee [5] reported an investigation that has been carried out on the neutron transmission through a PG filter as a function of the filter orientation with respect to the beam. It is shown that highly aligned PG may be tuned for optimum scattering of second-order neutrons in the wave-length range between 1.12Å and 4.25Å, by adjusting the filter in an appropriate orientation.

The favorable properties of HOPG filters are to some extent offset by the fact that they only apply to a few discrete wave-length values. The range of applicability for a PG filter may be extended by *tuning* the filter appropriately. Tuning has been discussed previously [5] in connection with the required adjustment of the average *c*-direction parallel to the beam. The selective scattering of second-order neutrons is possible within a large, continuous wave-length range by choosing a proper orientation of the average *c*-direction with respect to the incident beam.

The present work concerns with the main features of the designed computer package GRAPHITE, which permits the calculation of the total graphite neutron cross-section for poly or pyrolytic graphite structure form

## THEORETICAL TREATMENT

The graphite absorption cross-section due to nuclear capture is very small ( $\approx 3$  mb at  $E_n = 0.025$  eV). Therefore the total cross-section determining the attenuation of neutrons is given by the sum:

$$\sigma = \sigma_{ids} + \sigma_{Bragg} \quad (1)$$

where,  $\sigma_{ids}$  is the thermal diffuse scattering and  $\sigma_{Bragg}$  correspond to Bragg scattering cross-section due to reflection from (*hkl*) planes.

As shown by Freund [6]  $\sigma_{ids}$  can be split into  $\sigma_{mph}$  (multiple phonon) and  $\sigma_{sph}$  (single phonon) depending on neutron energy.

The single phonon scattering cross-section, concerns the energy range  $E \ll K_B \theta_D$ , where  $K_B$  is Boltzmann's constant and  $\theta_D$  is the Debye temperature characteristic of the graphite. The second part of TDS is predominant in the range  $E \geq K_B T$  where down scattering and multiphonon processes occur. As shown by Freund [6], the predicted empirical equation for  $\sigma_{mph}$  fits the experimental results rather well except for graphite.

However, using the static incoherent approximation Cassels [7] has estimated the short-wavelength elastic cross-section. Hence the multiphonon scattering cross-section term given by Freund [6] in the range  $E \gg K_B \theta$  can be replaced by :

$$\sigma_{mph} = \sigma_{free} \left\{ 1 - \left( \frac{\lambda^2}{2w} \right) \left[ 1 - \exp \left( - \frac{2w}{\lambda^2} \right) \right] \right\} \quad (2)$$

where,  $e^{-w}$  is the Debye-Waller factor [8] and  $\sigma_{free}$  is the free atom cross-section given as:

$$\sigma_{free} = \sigma_{bat} \frac{A^2}{(A+1)^2} \quad (3)$$

where  $\sigma_{bat}$  is the sum of the coherent and incoherent scattering cross-sections of the bound atom, and A is the atomic mass number

At each neutron wavelength the contribution of Bragg scattering cross-section to the total cross-section was calculated taking into consideration the crystalline form of graphite. The developed PCG, PG and HOPG codes for polycrystalline, PG at  $\psi = 0$  and HOPG at different angles  $\psi$  respectively. The Bragg scattering term  $\sigma_{Bragg}$  for each case is described below.

## COMPUTER PACKAGE GRAPHITE

Computer package GRAPHITE has been developed in order to calculate the total cross section and transmission of neutrons of energy range from 0.1meV to 10eV through crystalline graphite. The package includes three codes:PCG (Polycrystalline Graphite), PG (Pyrolytic Graphite) and. HOPG (Highly Oriented Pyrolytic Graphite). Each code includes two main subroutines, namely SATR and SCOH.

### SATR Subroutine

The SATR is used to calculate the  $\sigma_{tds}$  term as a function of neutron wavelengths in the range from 0.001nm up to 1.4nm with steps of 0.001nm. The equations and input graphite physical parameters used for calculation are taken the same in the three codes. Where the multi-phonon cross section term was calculated using Freund's formula and Cassels's one each in its given energy range.

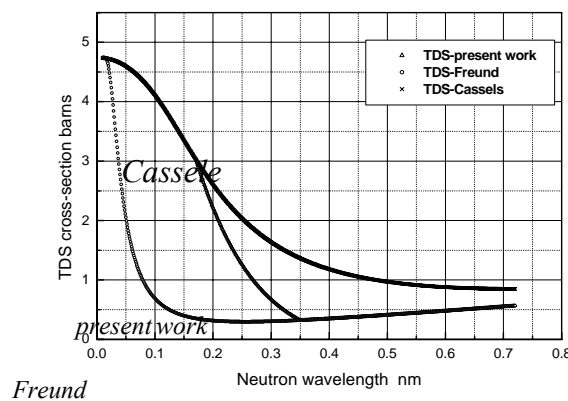


**Figure 1.** The TDS cross-section versus neutron wavelength.

While, the single phonon term was calculate as given by Freund [6] for  $\theta_D/T < 6$  and for  $\theta_D/T > 6$  the Bernoulli series is replaced by a  $T^{-7/2}$  law and a term of  $(T/\theta_D)^{-2.25}$  accounting for low energy excitations occurring in  $\mu\text{eV}$  region is added.

The TDS cross-section of graphite as a function of neutron wavelength was calculated using Freund's and Cassels's formula and displayed in Fig(1).using the graphite physical parameters listed in Table 1. The TDS cross-section using both formulas were found converge at  $\lambda > 0.7\text{nm}$ , while strongly diverges at  $\lambda < 0.4\text{nm}$ . The comparison of the calculated values of TDS with the experimental ones in the wavelength range where the reflections from  $(hkl)$  is absent, show an agreement with Cassels's formula for neutrons with  $\lambda < 0.15\text{nm}$  and with Freund's for neutrons with  $\lambda > 0.35$ . The values of TDS in the wavelength band  $0.15\text{nm} < \lambda < 0.35\text{nm}$  were fitted to the available experimental data.

The equation:  $\sigma_{TDS} = \frac{\lambda^F - \lambda}{\lambda^F - \lambda^C} \sigma_{TDS}^C + \frac{\lambda - \lambda^C}{\lambda^F - \lambda^C} \sigma_{TDS}^F$  was found to be the best fit to the experimental data for neutrons with wavelengths between  $\lambda^C = 0.17\text{nm}$  and  $\lambda^F = 0.35\text{nm}$ . The best fit is also displayed in Figure 1.

### SCOH Subroutine

At each neutron wavelength the contribution of Bragg scattering cross- section to the total cross-section  $\sigma_{Bragg}$  was calculated. Since  $\sigma_{Bragg}$  depends upon the crystalline form of graphite crystals, their mosaic spread and orientation with respect to the incident neutron beam, therefore PCG, PG and HOPG codes were developed for polycrystalline, PG at  $\psi = 0$  and HOPG at different angles  $\psi$  respectively.

However, at each wavelength step within the wavelength band of SATR subroutine, the structure factors for all  $(hkl)$  planes from  $(-15,-15,-15)$  to  $(+15,+15,+15)$  for the hexagonal closed packed graphite structure with four atoms were calculated the same in the three codes.

For each plane with non-zero structure factor the interplaner distances  $d_{hkl}$  were calculated. While, for calculation of Bragg scattering cross section  $\sigma_{Bragg}$  as function of neutron wavelength each code has its own SCOH subroutine.

### SCOH Subroutine in PCG code

The contribution of Bragg scattering  $\sigma_{Bragg}$  to the total cross section taking into account the resulting reflection from different  $(hkl)$  planes, which are able of giving the Bragg reflection for the neutron wavelength  $\lambda$  was calculated. In case of polycrystalline material the reflections are from all planes having spacing  $d_{hkl} \geq \lambda/2$ . The Bragg scattering cross-section was calculated using equation:

$$\sigma_{Bragg}(\lambda) = \frac{N_c \lambda^2}{2} \sum_{d_{hkl} \geq \lambda/2} F_{hkl}^2 d_{hkl} e^{-2w} \quad (4)$$

where  $N_c$  is the number of unit cells per cubic centimeter,  $F_{hkl}$  is the structure factor of the unit cell and  $e^{-2w}$  is the Debye-Waller factor.

### SCOH Subroutine in PG code

When a PG plate is oriented with the c-direction parallel to the incident neutron beam, a strong attenuation due to coherent elastic scattering by the  $(hkl)$  planes will occur if neutron wavelength satisfies the Bragg condition  $\lambda = 2 d_{hkl} \sin \theta_{hkl}$

The planes  $(00l)$ , on the other hand, scatter neutrons with a discrete wavelength  $\lambda = 2 d_{00l}$  The Bragg scattering cross-section of PG crystal due to reflection from  $(00l)$  planes is given by:

$$\sigma_{Bragg} = \sigma_{Bragg}(00l) + \sigma_{Bragg}[non - (00l)] \quad (5)$$

The Bragg scattering due to reflection from  $(00l)$  planes is given by Naguib et al. (1996)

$$\sigma_{Bragg}^{(ool)} = -\frac{1}{N t_o} \ln(1 - P_{(ool)}) \quad (6)$$

Where  $N$  is the number of atoms/cm<sup>3</sup>,  $t_o$  is the effective thickness of the crystal in cm and  $P_{(ool)}$  is the reflecting power of the  $(00l)$  plane perpendicular to the incident beam direction where  $P_{(ool)}$  for zero absorption cross section is given by

$$P_{(ool)} = \left[ \left( \frac{Q t_o}{\gamma} \right) W(\Delta) / \left\{ 1 + \left( \frac{Q t_o}{\gamma} \right) W(\Delta) \right\} \right] \quad (7)$$

where  $Q$  is the well-known crystallographic quantity,  $W(\Delta)$  is the Gaussian distribution of the graphite mosaic blocks.

While the Bragg scattering cross-section due to scattering neutrons from a non- $(00l)$  plane at  $\lambda$  and can be given as

$$\sigma_{Bragg} = N(\lambda, hkl) F_{hkl}^2 e^{-2w} \quad (8)$$

Where is  $N(\lambda_{hkl}, hkl)$  the number of crystallites at  $\lambda_{hkl}$ .

As shown by Frikkee [5],  $N(\lambda_{hkl}, hkl)$  is inversely proportional to  $\sqrt{\cos \theta_{hkl}}$  and reaches pronounced maximum at  $\lambda = \lambda_{hkl}$ . Therefore the Bragg scattering cross-section due to reflection from non- $(00l)$  planes at  $\lambda$  satisfying Bragg equation and broadened by both mosaic spread and neutron beam divergence can be given as:

$$\sigma_{Bragg}^{non-(00l)} = N(\lambda_{hkl}, hkl) F_{hkl}^2 d_{hkl} e^{-2w} W(\Delta) \quad (9)$$

From all non- $00l$  planes with non-zero structure factor, where each peak due reflection from non- $00l$  is broadened by Gaussian distribution of the graphite mosaic blocks in similar very as for  $00l$ . Therefore the total Bragg scattering cross-section is given as:

$$\sigma_{Bragg} = \sigma_{Bragg}^{00l} + \sum_{hkl} \sigma_{Bragg}^{non-00l}$$

### SCOH Subroutine in HOPG

When a PG plate is oriented with the c-direction parallel to the incident neutron beam, a strong attenuation due to coherent elastic scattering by the  $(hkl)$  planes will occur if the neutron wavelength satisfies the Bragg condition:

$$\lambda = 2d_{hkl} \sin \theta_{hkl}. \quad (10)$$

If this angle is denoted by  $\psi$ , and if the mosaic spread is negligible in comparison with  $\psi$ , the lattice planes  $(hkl)$  will scatter neutrons in the following wavelength intervals:

$$\begin{aligned} 2d_{hkl} \sin(\theta_{hkl} - \psi) \leq \lambda \leq 2d_{hkl} \sin(\theta_{hkl} + \psi) & \quad \text{for } \theta_{hkl} \geq \psi \\ 0 \leq \lambda \leq 2d_{hkl} \sin(\theta_{hkl} + \psi) & \quad \text{for } \theta_{hkl} \leq \psi \end{aligned}$$

The planes  $(00l)$ , on the other hand, scatter neutrons with a discrete wavelength  $\lambda = 2d_{00l} \cos \psi = 2d_{00l} \sin \theta$  where  $\theta$  is the glancing angle

The Bragg scattering from  $(00l)$  planes are calculated in similar way as given in case when neutrons incident along c-direction.

The Bragg scattering cross-section due to reflection from non- $00l$  planes of a PG crystal with mosaic  $\eta$  and set at angle  $\psi$ , at wavelength  $\lambda$  in the interval between  $\lambda^-$  and  $\lambda^+$ , can be given as

$$\sigma_{Bragg}^{non-00l} = \frac{N_o \lambda^3 F_{hkl}^2 e^{-2w}}{4d_{hkl} \sin \psi \cos \theta_{hkl} \left| \lambda - \lambda_{hkl}^\pm \right|^{\frac{1}{2}}} \quad (11)$$

where  $\lambda^- = 2d_{hkl} \sin(\theta_{hkl} - \psi)$  and  $\lambda^+ = 2d_{hkl} \sin(\theta_{hkl} + \psi)$

While at boundaries i.e at  $\lambda^+$  and  $\lambda^-$  the Bragg scattering cross-section is broadened by mosaic spread  $W(\Delta)$  and can be expressed as

$$\sigma_{Bragg}^{non-00l} = \frac{N_o \lambda^3 F_{hkl}^2 e^{-2w} W(\Delta)}{4d_{hkl} \sin \psi \cos \theta_{hkl} (\delta\lambda)^{\frac{1}{2}}}$$

Where  $\delta\lambda$  is step of the wavelength spread.

Consequently, the Bragg scattering of PG crystal set at angle  $\psi$  versus wavelength due to reflections from  $(hkl)$  planes can be given as:

$$\sigma_{Bragg} = \sigma_{Bragg}^{00l} + \sum_{hkl} \sigma_{Bragg}^{non-00l} \quad \{12\}$$

where the summation is taken over all non- $(00l)$  planes satisfying the inequalities given by (5).

To show the effect of peak broadening of neutrons reflected from  $00l$  planes due to PG crystal mosaic spread, the calculation were carried out using HOPG code when 1cm thick PG crystal set at  $\psi=15^\circ$  assuming that the FWHM of its mosaic spread were  $1.0^\circ$  and  $0.4^\circ$ . The result of calculation is displayed in Fig(2). One can notice that the peaks are symmetric and tend to be sharper and higher with decreasing the crystal mosaic spread.

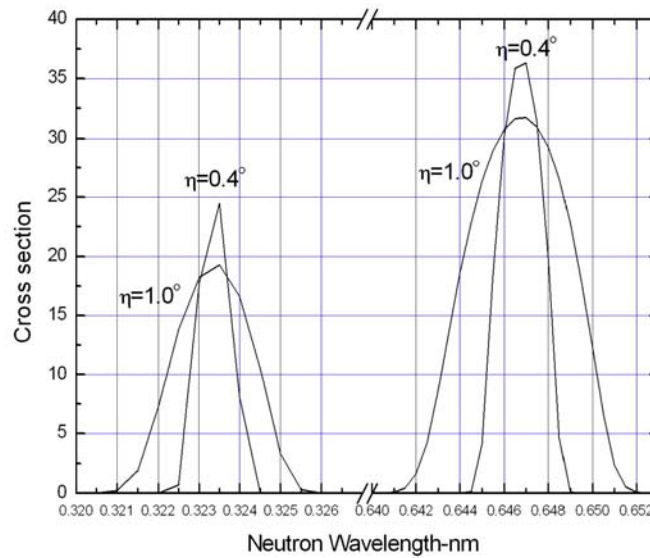


**Figure 2.** Reflection from  $00l$  planes.

Similar calculations were carried out when the PG crystal was set at  $\psi=55^\circ$  assuming that the reflection are only from planes with Miller indices  $hkl$  where  $h, k$  and  $l$  are  $\leq 1$ . The result of the total cross-section of 1cm PG crystal with  $1.0^\circ$  FWHM mosaic spread is displayed in Fig(3). It is apparent that the sharp boundaries at  $\lambda_{101}^+$ ,  $\lambda_{100}$  and  $\lambda_{110}$  are broadened by Gaussian distribution of PG mosaic blocks while decreasing as given by Eq.(11) in the wavelength range between  $\lambda_{101}^-$  and  $\lambda_{101}^+$  while from 0 to  $\lambda_{hk0}$  for 110 and 100. Such cross section plane behaviors was found to be in agreement with the experimental results carried out by Mildner [9]

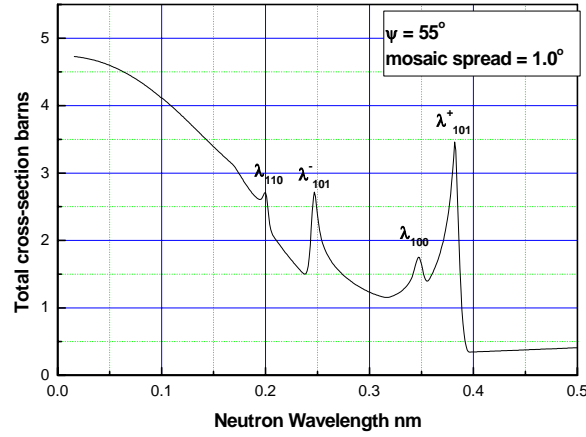


**Figure 3.** Reflection from 101 planes at  $\psi=55^\circ$

The main computer package GRAPHITE flow charts are given in the Appendix.

### Comparison with experimental results and discussions

The main graphite physical parameters required in calculations are listed in Table 1.

**Table 1.** Physical parameters of graphite.

Atomic weight	12
Crystal structure	HCP
Space group	P63/mmc (Nr.94)
Lattice parameters	$a = 0.2456 \text{ nm}$ $c = 0.6696 \text{ nm}$
Atomic positions	4 atoms / unit cell $0,0,0 ; 0,0,\frac{1}{2} ; \frac{2}{3},\frac{1}{3},0 ; \frac{1}{3},\frac{2}{3},\frac{1}{2}$
Number of unit cells / $\text{m}^3$	$0.284 \text{ E}29$
Coherent scattering length $b_c$	6.61 fm
Absorption cross-section $\sigma_a$ ( $E = 0.025$ )	0.0035 barn
Total scattering cross-section ( $\sigma_{bat}$ )	5.551 barn
Debye temperature	1050 K

### Neutron transmission through Polycrystalline Graphite

Using PCG code, the total cross-section of graphite at temperatures of 300K and 478K were calculated for neutrons in the energy range from 0.1meV up to 1eV. The results of calculation are displayed in Figure 7, as solid lines. For comparison, the experimental data [10] measured at ET\_RR-1 reactor using the time-of-flight spectrometer are also displayed in Figure 4 as open circles and closed circles at 300K and 474K respectively. The calculated data are almost in agreement with experimental values for the fitted parameters  $C_2=5.0$  and  $\theta_D=1050\text{K}$ . From Figure 4, one can observe that the graphite total cross-section beyond the cut-off wavelength ( $\lambda_c=2d_{002}$  i.e. at  $E < 1.8\text{meV}$ ) is about 0.6 barn. This value is much less than the free atomic cross-section  $\sim 4.7$  barns at neutron energies higher than 1eV.

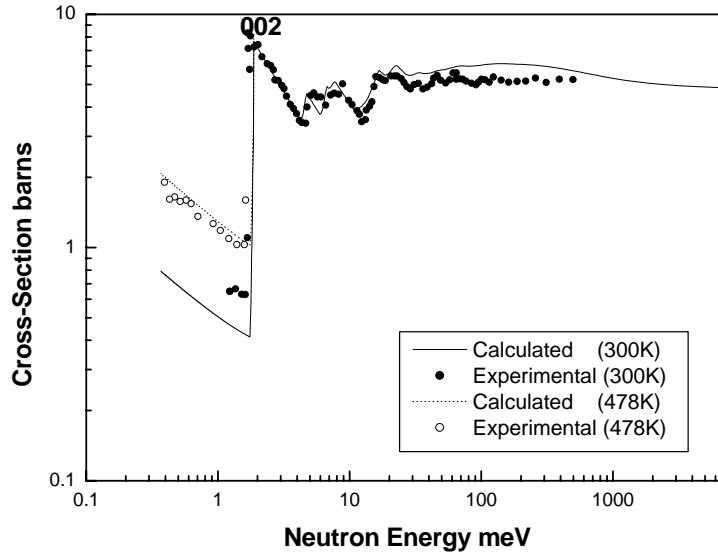


**Figure 4.** Total Neutron Cross-section for Polycrystalline Graphite.

Such cross section difference justifies the use of polycrystalline graphite as a high efficient cold neutron filter for neutrons with wavelengths longer than 0.67nm ( $E=1.8\text{meV}$ ).

#### Transmission through PG for Neutrons Incident Along C-Direction

The total cross-section data of PG reported by Loopstra [11] for neutrons incident along the average direction of alignment of the c-axis is displayed in Fig(5) as closed circles. The PG used in this investigation consists of plates of 2"x 2"x 3/8" in which the c-axes were aligned to within  $5^\circ$  from the normal of the largest face. The calculated values using PG code and physical parameter listed in Table(4) are also displayed in Fig(5) as solid line, assuming that PG has standard deviation of mosaic spread 0.037 Radian (i.e. FWHM =  $5^\circ$ ). The best fit with the experimental data was obtained when  $\sigma_{ids}$  was calculated using Freund's [6] formula for neutron energies  $E < 0.2 \text{ eV}$  while, Cassels's [7] one for  $E > 0.2 \text{ eV}$ .

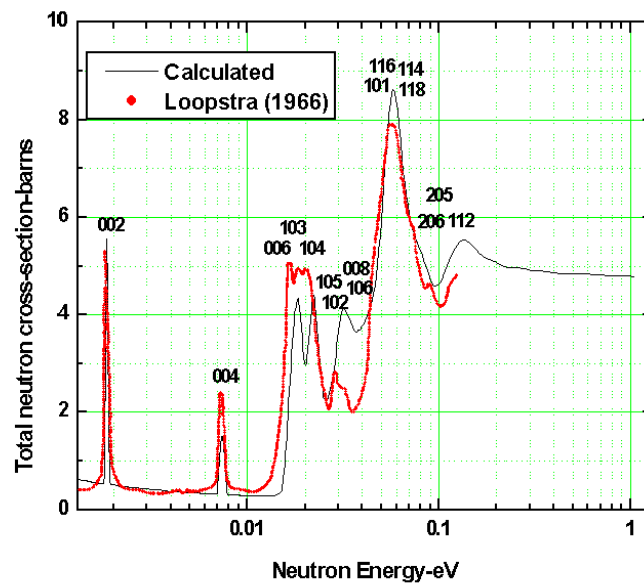


**Figure 5.** Total cross-section of PG crystal for neutrons incident along its c-axis.



The calculated cross-section values due to reflection from  $(00l)$  are in reasonable agreement with measured ones. While the observed slight disagreement from non- $(00l)$  planes may be due to the divergence of  $N(\lambda_{hkl}, hkl)$  at  $\lambda_{hkl}$ , as predicted by Frikkee[6]

### Neutron Transmission through HOPG set at different Angles.

The values of wavelengths for various reflections  $(hkl)$  having non-zero structure factor and for different PG crystal setting angle  $\theta$  relative to the incident beam are calculated using HOPG code. The result of calculations is listed in Table 6 along with the calculated values reported by Mildner [9]. Where the angle  $\theta$  is the complementary angle of  $\psi$ .

The good agreement obtained between both sets of calculations supports the application of HCP structure with four atoms per graphite unit cell. However the wavelength value at which the reflection from (111) plane occur is not included in our calculation since it has a zero structure factor.

Mildner [9] has performed neutron transmission measurements through a  $0.4^\circ$  mosaic pyrolytic graphite monochromator crystal set to diffract thermal neutrons at different wavelengths. The measurements were performed on the C3 beamline, used for the time-of-flight small-angle neutron diffractometer SAND at the Intense Pulsed Neutron Source at Argonne National Laboratory.

Data were collected with the graphite monochromator crystal set at nominal angles of  $90, 45, 32$  and  $22^\circ$  to the incident beam, so that the 002 reflection corresponded to diffraction in the horizontal plane at wavelengths,  $\lambda$ , of  $0.6696, 0.4735, 0.3548$  and  $0.2508$  nm, respectively. The operating program of the instrument bins the data for each monitor detector into variable time  $\tau$  channels commensurate with those for the position-sensitive area detector of the diffractometer, which for these measurements were set to a time resolution of 2%, or  $\Delta\lambda/\lambda = 2\%$ .

**Table 6.** Calculated wavelengths (nm) for various reflections  $(hkl)$  and for different crystal setting

hkl	$\psi = 0^\circ$ ; $\Theta = 90^\circ$		$\psi = 45^\circ$ $\Theta = 45^\circ$		$\psi = 58^\circ$ $\Theta = 32^\circ$		$\psi = 68^\circ$ $\Theta = 22^\circ$	
	Present work $\lambda$ -nm	Mildner $\Lambda$ -nm	Present work $\lambda$ -nm	Mildner $\lambda$ -nm	Present work $\lambda$ -nm	Mildner $\lambda$ -nm	Present work $\lambda$ -nm	Mildner[] $\lambda$ -nm
002	0.6695	0.6696	0.473	0.4735	0.335	0.3348	0.251	0.2508
004	0.3348	0.3348	0.237	0.2367	0.177	0.1774	0.125	0.1254
006	0.2232	0.2232	0.158	0.1578	0.118	0.1183	0.084	0.0836
008	0.1674	0.1674	0.118	0.1184	0.089	0.0887	0.063	0.0627
100	----	----	0.3008	0.3008	0.3608	0.3608	0.3944	0.3944
101	0.1227	0.1227	0.3600	0.3600	0.3927	0.3927	0.4042	0.4043
102	0.1925	0.1925	0.3505	0.3505	0.3591	0.3591	0.3531	0.3531
103	0.2124	0.2125	0.3079	0.3079	0.3016	0.3017	0.2863	0.2863
104	0.2067	0.2060	0.2612	0.2612	0.2475	0.2475	0.2283	0.2283
105	0.1918	0.1918	0.2210	0.2210	0.2041	0.2041	0.1838	0.1838
106	0.1750	0.1750	0.1887	0.1887	0.1706	0.1706	0.1507	0.1507
110	----	----	0.1737	0.1736	0.2083	0.2082	0.2277	0.2278
111	----	0.0436	----	0.1148	----	0.1238	----	0.1265
112	0.0794	0.0794	0.2092	0.2060	0.2257	0.2230	0.2305	0.2305

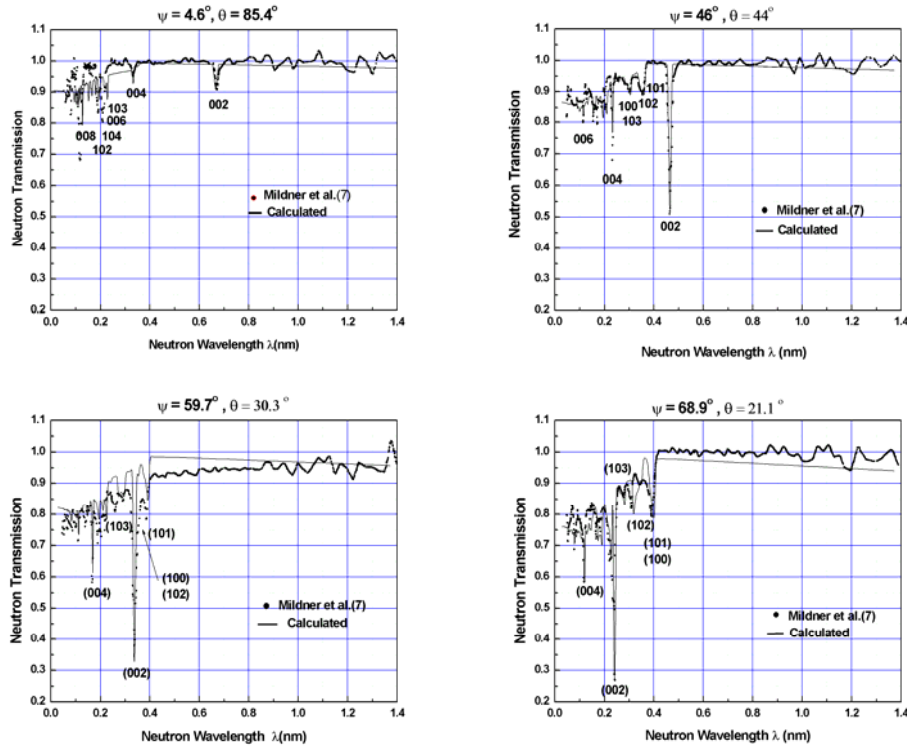


**Figure 6.** Transmission results for PG set at different angles.

An overall agreement was obtained between the calculated neutron transmissions and measured ones at longer wavelengths ( $>5$  nm) for different angles. However, the slight disagreement observed may be due to the lack of the experimental transmission data through such thin HOPG crystal used by Mildner [9]. Where the transmission at some wavelengths exceed one. Such inconsistent at  $\theta = 30.3^\circ$  is also observed by Mildner [9]. They reported that, they have no adequate explanation for this.

The calculated position and depth of the major Bragg dips in the transmission caused by various  $(hkl)$  reflections are found to be in good agreement with the measured ones. Such agreement supports the application of the HOPG code for calculations. From Fig.6 one can note that at shorter wavelengths, in the region where the non-00 $l$  reflections are available, the transmission is reduced considerably. For small  $\theta$  settings, the 10 $l$  reflections with their broad asymmetric dips in the transmission occur at wavelengths longer than the 002 reflection, whereas the opposite is true for the larger  $\theta$ .

## CONCLUSIONS

The developed computer package GRAPHITE permits the calculation of the total cross-section, neutron transmission and removal coefficient of crystalline graphite in the energy range from 0.1meV up to 10eV within an accuracy which is sufficient for determining the validity of the graphite crystal when it used as neutron filter.

The package is based on calculation of TDS  $\sigma_{tds}$  cross-section in a similar way regardless the crystalline form of the graphite.

The main physical graphite parameters required in these calculations are taken from the Nuclear Data Library. While the fitting parameters  $C_2$  and  $\theta_D$  were deduced from the measured neutron cross-section of graphite in various crystalline form in the energy range where the Bragg scattering reflections are not allowed. The best fit with the experimental data was obtained for  $C_2 = 5 \text{ \AA}^{-2} \cdot \text{eV}^{-1}$  and  $\theta_D = 1050 \text{ K}$ . Moreover  $\sigma_{tds}$  was calculated using Freund's

formula for neutron energies  $\lambda < 0.35\text{nm}$  while Cassels's ones for  $\lambda > 0.15\text{nm}$  and a average mean value between  $0.15\text{nm}$  and  $0.35\text{nm}$ .

The computer SCOH subroutine in the codes PCG, PG and HOPG included in the GRAPHITE package are developed for the calculation of the contribution of the Bragg scattering  $\sigma_{\text{Bragg}}$  to the total cross section due to all possible Bragg reflections from polycrystalline graphite, PG when neutrons incident along c-axis and HOPG set at different angles respectively.

The good agreement obtained between, the calculated Bragg scattering cross-section values of wavelengths of various  $hkl$  reflections having non-zero structure factor from different graphite crystals with the experimental ones supports the application of the HCP structure with four atoms per graphite unit cell.

The computer package GRAPHITE have been successfully applied for the feasibility study on using a polycrystalline graphite as , a cold neutron filter PG crystals as efficient second order filter. The results of these studies are reported elsewhere [12-14].

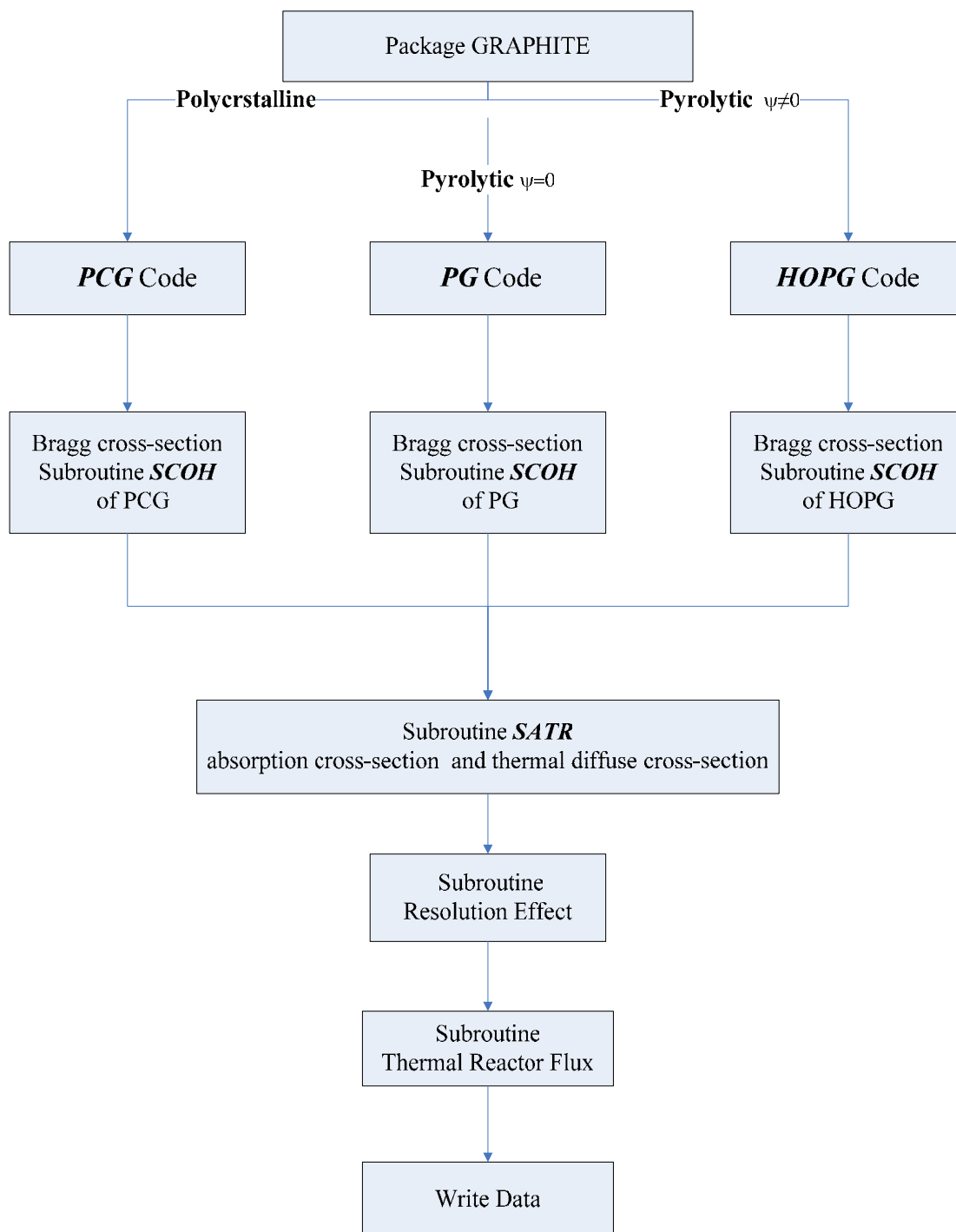
## REFERENCES

- [1] Bacon G.E. ; Neutron Diffraction 3<sup>rd</sup> Edn. Claredon, Oxford (1973).
- [2] Kasivz, G., Treatise on Material Science and Technology, Academic Press., Institute Lawe-Langevin, Grenoble, France (1979).
- [3] Torchin, V.F., Cold Neutrons, Gosatomezdat Press, Moscow (1963).
- [4] Duggal, V.P., and Thaper, C.L., Rev. Sci. Instrum, 33, 49 (1962).
- [5] Frikkee, E. , Nucl. Instr. and Meth. No. 125, (1975) pp.307-312
- [6] Freund ,A.K. : Nucl. Inst. Meth. 213 (1983) p.1553.
- [7] Cassels , J.M., Prog. Nucl. Phys. 1, (1950) p. 185
- [8] Bacon, G.E. Neutron Diffraction 3rd Edn. Oxford Claredon Oxford (1975)pp.
- [9] Mildner, D.F.R., Arif, M. and Werner, S.A.. J. Applied Crystallography 34, (2001). pp.255-262.
- [10] Kilany, M. M.Sc. Thesis, 'Interaction of thermal and cold neutrons with solids' Faculty of women, Ain Shams University (1986).
- [11] Loopstra, B.O., Nucl. Instrum. and Methods. No. 44 (1966) pp.181-186
- [12] Adib, M., Ismaail, H., Abbas, Y. , Habib, N., Wahba, M., and Fathalla, M., "Attenuation of Thermal Neutron Through Graphite". Proc. 4<sup>th</sup> Conf. on Nuclear and Particle Physics 11-15 Oct., 2003 (Ed. Prof. Comsan). Egyptian Nuclear Physics Association. Cairo, August 2004., pp. 257-269
- [13] Adib, M., Habib, N. and Fathalla ,M.. Annals of Nuclear Energy 33(2006)pp.627-632
- [14]. Adib , M., Habib, N. and Fathalla ,M. Ukraine Journal of Nuclear Physics and Atomic Energy 2,18(2006)

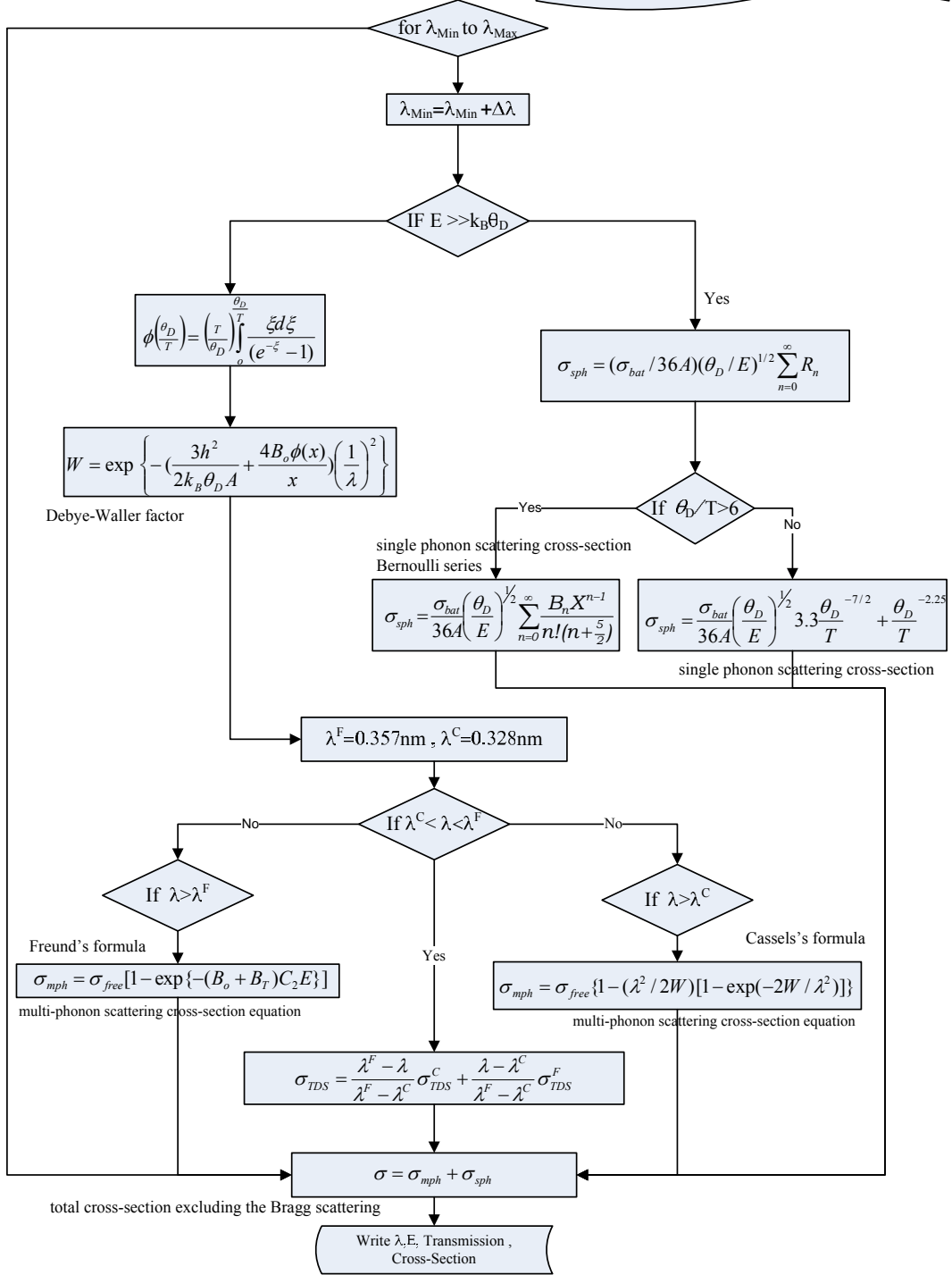
## APPENDIX

### Computer Package GRAPHITE Flowchart

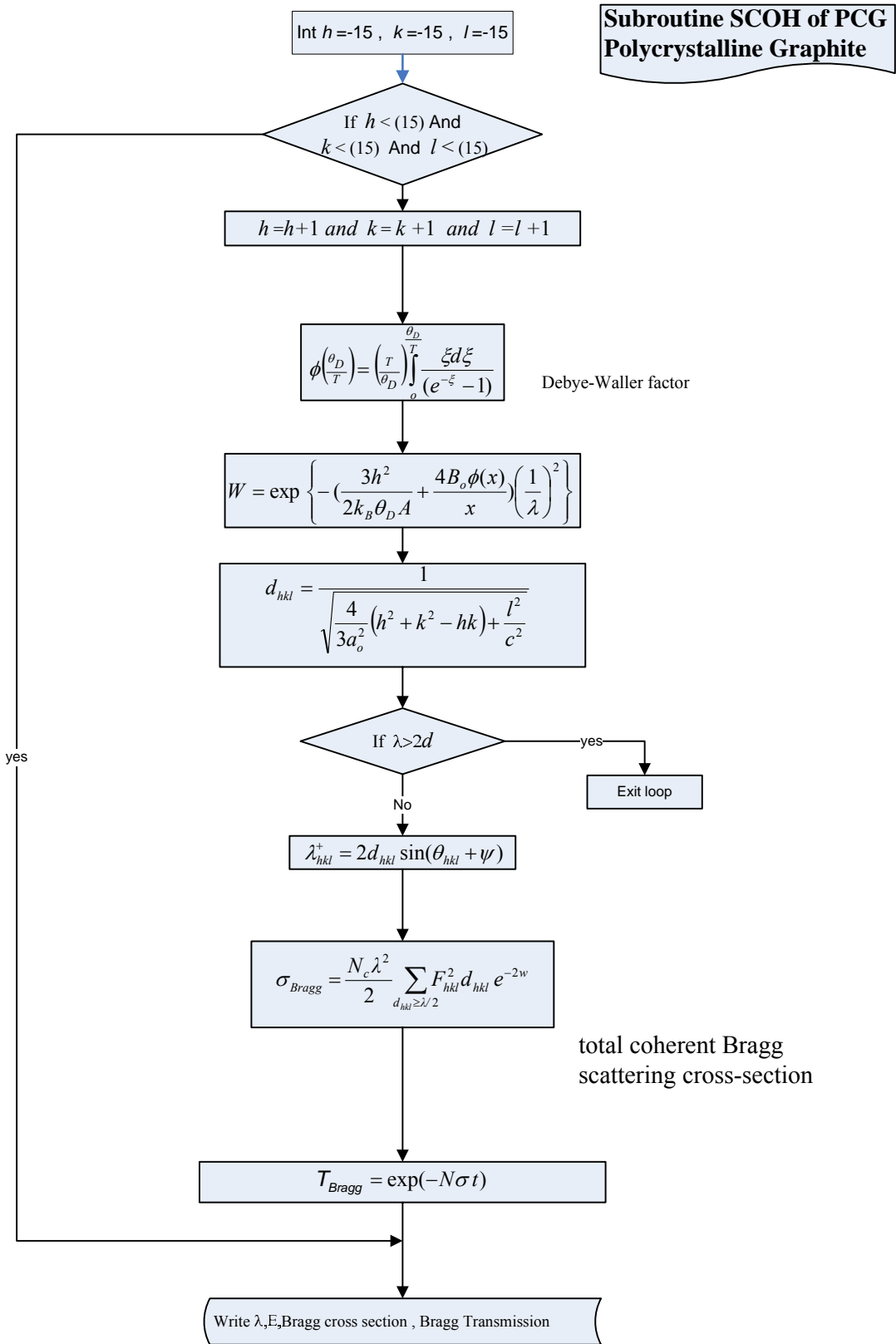
The schematic diagram of the computer package GRAPHITE for graphite cross-section calculation is presented in flowchart 1.



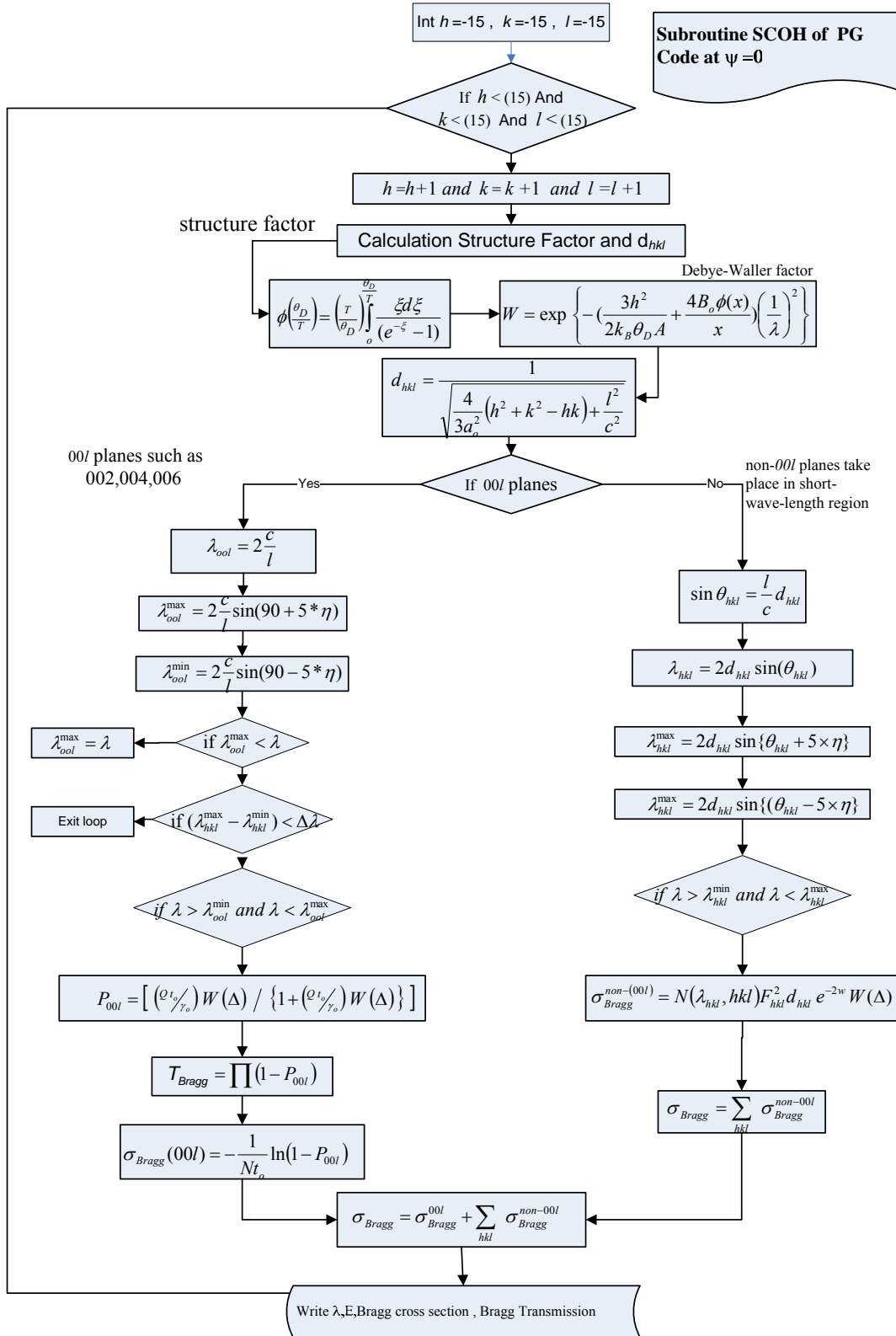
**Flowchart 1.** Schematic diagram of Computer package GRAPHITE



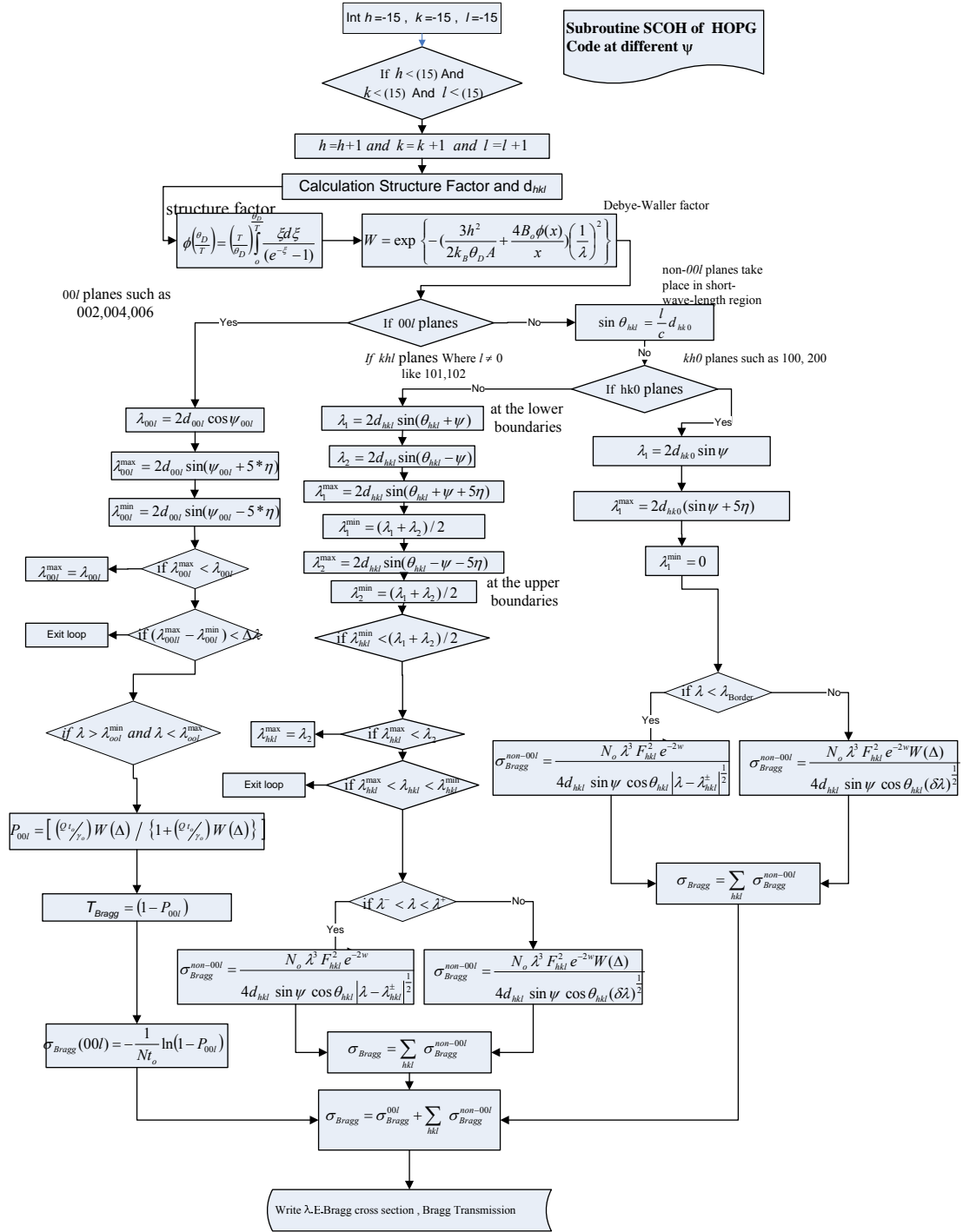
**Flowchart 2.** Subroutine *SATR*



**Flowchart 3.** Subroutine SCOH of PCG Polycrystalline Graphite



**Flowchart 4.** Subroutine SCOH of PG Code at  $\psi=0$



**Flowchart 5.** Subroutine SCOH of HOPG Code at different  $\psi$  □